Title

Integration of Stress Signaling in Caenorhabditis elegans Through Cell Non-autonomous Contributions of the JNK Homolog KGB-1

Journal

Genetics, 210(4)

ISSN

0016-6731

Authors

Liu, Limeng
Ruediger, Cyrus
Shapira, Michael

Publication Date

2018-12-01

DOI

10.1534/genetics.118.301446

Peer reviewed

Integration of Stress Signaling in *Caenorhabditis elegans* Through Cell-Nonautonomous Contributions of the JNK Homolog KGB-1

Limeng Liu,[1] Cyrus Ruediger, and Michael Shapira[2]
Department of Integrative Biology, University of California at Berkeley, California 94720
ORCID ID: 0000-0003-1332-2220 (M.S.)

ABSTRACT Dealing with physiological stress is a necessity for all organisms, and the pathways charged with this task are highly conserved in Metazoa . Accumulating evidence highlights cell-nonautonomous activation as an important mode of integrating stress responses at the organism level. Work in *Caenorhabditis elegans* highlighted the importance of such regulation for the unfolded protein response (UPR) and for gene expression downstream of the longevity-associated transcription factor DAF-16. Here we describe a role for the JNK homolog KGB-1 in cell-nonautonomous regulation of these two response modules. KGB-1 protects developing larvae from heavy metals and from protein folding stress (which we found to be independent of canonical UPR pathways), but sensitizes adults to the same stress, further shortening life span under normal conditions. This switch is associated with age-dependent antagonistic regulation of DAF-16. Using transgenic tissue-specific KGB-1 expression or tissue-specific KGB-1 activation we examined the contributions of KGB-1 to gene regulation, stress resistance, and life span. While cell-autonomous contributions were observed, particularly in the epidermis, cell-nonautonomous contributions of neuronal KGB-1 (and also in muscle) were effective in driving intestinal gene induction, age-dependent regulation of intestinal DAF-16, and stress resistance, and did not require KGB-1 expression in the target tissue. Additional genetic analyses revealed requirement for UNC-13 in mediating neuronal contributions, indicating involvement of neurotransmission. Our results expand the role of KGB-1 in stress responses from providing local cellular protection to integrating stress responses at the level of the whole organism.

KEYWORDS *Caenorhabditis elegans*; KGB-1; autonomous; nonautonomous; DAF-16; stress

STRESS typically does not target a single cell, but rather a tissue, or even the whole organism. This is obvious in the case of environmental stress, such as heat, exposure to environmental toxins, or infection. It is also frequently true for endogenously initiated stress, such as malfunctions leading to protein aggregation, or the release of reactive oxygen species by immune cells (Walsh and Selkoe 2016; Winterbourn *et al.* 2016). However, different cells may respond differently to stress, and may vary in their inherent resistance. Furthermore, different tissues may be more exposed to certain types of stress than others, such as the skin to UV radiation or the intestine to food-derived toxins and pathogens, and the susceptibility of certain tissues may affect the entire organism. Thus, whereas different cells rely on similar stress response mechanisms, the function and contribution of these pathways to stress resistance and organismal survival may differ between different cells and tissues.

Stress-activated MAP kinases are among the most central and evolutionary conserved mechanisms responding to cellular stress in Metazoa. They include the p38 kinase and the c-Jun N-terminal kinase (JNK), each represented by several isoforms, and together contributing to protection from adverse conditions including protein folding stress, oxidative stress, DNA damage, and infection (Kyriakis and Avruch 2001). *Caenorhabditis elegans* has three homologs each of p38 and JNK kinases. Well-characterized members of these

doi: https://doi.org/10.1534/genetics.118.301446
Manuscript received March 30, 2018; accepted for publication September 25, 2018; published Early Online October 5, 2018.
Supplemental material available at Figshare: https://doi.org/10.25386/genetics.7159487.v1.
[1]Present address: State Key Laboratory of Molecular Developmental Biology, Institute of Genetics and Developmental Biology, Chinese Academy of Sciences, 100101 Beijing, China.
[2]Corresponding author: Valley Life Sciences building, room 5155., University of California at Berkeley, Berkeley, CA 94720. E-mail: mshapira@berkeley.edu

families are the p38 PMK-1, which provides protection from oxidative stress and infection resistance, and the JNK homolog KGB-1, which provides protection from protein folding stress (ER stress) and from heavy metals (Kim *et al.* 2002; Mizuno *et al.* 2004; Inoue *et al.* 2005). The dual-specificity phosphatase, VHP-1/DUSP8, negatively regulates both PMK-1 and KGB-1, enabling tight control over their activity (Kim *et al.* 2004; Mizuno *et al.* 2004). Previous work in our laboratory identified an age-dependent reversal in the contribution of KGB-1: from protective in larvae against protein folding stress and heavy metals, to detrimental in adults, increasing susceptibility to these stressors as well as to infection, and further shortening life span (Twumasi-Boateng *et al.* 2012). This reversal was associated with age-dependent antagonistic regulation of the stress resistance and longevity-associated transcription factor DAF-16/FOXO, whose nuclear localization was promoted by KGB-1 activation in larvae, but attenuated in adults. A second transcription factor, FOS-1, a component of the AP-1 heterodimer, was also found to mediate effects of KGB-1 activation on gene expression, but unlike DAF-16, FOS-1 involvement was age-invariant and did not directly affect stress resistance (Zhang *et al.* 2017). Others have shown that the KGB-1/AP-1 module extended life span following intermittent fasting (Uno *et al.* 2013).

How KGB-1 contributes to stress resistance, and in which tissue(s), is not well understood. In the epidermis of developing worms with disrupted KGB-1 signaling, restored KGB-1 activation, achieved by epidermis-specific expression of the MAPK kinase MEK-1 and the scaffold protein SHC-1, was sufficient to promote heavy metal resistance, suggesting a role for epidermal KGB-1 (Mizuno *et al.* 2008). In turn, it may be hypothesized that intestinal KGB-1 activation plays a role in the detrimental contributions in adults to infection resistance and life span, as the intestine is the site of infection (Twumasi-Boateng and Shapira 2012; Block *et al.* 2015), and is a tissue shown to be important for regulation of longevity (Libina *et al.* 2003).

Here, we characterize the tissue-specific contributions of KGB-1. KGB-1 was found to be broadly expressed, including in the pharynx, intestine, epidermis, muscle, as well as in a subset of neurons. Tissue-specific expression of KGB-1, or tissue-specific activation, demonstrated both cell-autonomous and -nonautonomous contributions of KGB-1 to gene expression, stress resistance, and life span. While epidermal stress responses appeared to be local, the majority of KGB-1's contributions, including its age-dependent regulation of intestinal DAF-16, could be activated cell-nonautonomously by neuronal or muscle KGB-1. Additional genetic analyses identified a role for neurotransmitter secretion in mediating neuronal contributions. The newly identified cell-nonautonomous functions of KGB-1 provide a means for integrating stress responses at the level of the whole organism, and expand its known roles in such responses.

Materials and Methods

Strains

KU21 (*kgb-1(km21)*), TJ356 (*zIs356* [*daf-16p*::*daf-16a/b*::*GFP* + *rol-6(su1006)*]), BC14229 (*dpy-5(e907)*; *sEx14229* [*cpr-3p*::*GFP* + *dpy-5*]), SJ4005 (*zcIs4 [hsp-4*::*GFP]*), RB772 (*atf-6(ok551)*), RB545 (*pek-1(ok275)*), WM27 (*rde-1(ne219)*), NR222 (*rde-1 (ne219)*;*kzIs9*[(pKK1260)*lin-26p*::*NLS*::*GFP* + (pKK1253)-*lin-26p*::*rde-1* + *rol-6(su1006)*]), and N2 wild-type strains were obtained from the *Caenorhabditis* Genetics Center (Minneapolis, MN). Strains CB928 (*unc-31(e928)*), CB450 (*unc-13(e450)*), *xbp-1(zc12)*, HC196 (*sid-1(qt9)*, and AGD637 (*sid-1*(*qt9*);*uthIs201*[*rab-3p*::*sid-1*::*unc-54 3′UTR*; *rab-3p*::*tdTomato*::*unc-54 3′UTR*]) were gratefully received from the laboratory of Andrew Dillin, at the University of California Berkeley. MGH167 (*sid-1*(*qt9*); *alxIs9*[*vha-6p*::*sid-1*::*SL2*::*GFP*]) was gratefully received from Alex Soukas, Harvard Medical School. Strains containing combinations of the aforementioned mutations and transgenes were generated by mating and verified by PCR and sequencing.

Bacterial strains included *Escherichia coli* OP50-1, and *Pseudomonas aeruginosa* PA14 (Shapira and Tan 2008).

Transgenic animals

kgb-1p::kgb-1::gfp transgenic animals: A total of 8718 bp of the *kgb-1* locus, including 4635 bp of the sequence upstream to *kgb-1* transcription start site, and the entire coding sequence excluding the stop codon, were amplified from genomic DNA using primer A (5′-CAGGTTTGCCAACAGTTGTTTA-3′) and a tailed primer B (5′-agtcgacctgcaggcatgcaagcttCCAGT GAAAATGTCGTGGTC-3′). A second fragment including GFP and the unc-54 3′UTR was amplified from Addgene plasmid L3787 (#1594), using primers C (5′-AGCTTGCATGCCTG CAGGTCG-3′) and D (5′-AAGGGCCCGTACGGCCGACTA-3′) (Boulin *et al.* 2006), and the two fragments were fused using recombinant PCR with nested primers A* (5′-TCTCGAAGTGT TAGAAGCACCA-3′) and D* (5′-GGAAACAGTTATGTTTGG TATA-3′). The obtained *kgb-1p*::*kgb-1*::*gfp* transgene was co-injected with the *rol-6(su1006)* marker into *kgb-1(km21)* mutants. Transgene integration following UV irradiation, and backcrossing to wild-type animals, leads to generation of both *kgb-1* mutants carrying the transgene, as well as the wild-type animals carrying the same transgene described in this study.

Tissue-specific kgb-1 transgenic worms: Tissue-specific *kgb-1* expression was driven by previously described promoters, including the intestinal *gly-19*, muscle *myo-3*, neuronal *rgef-1*, and hypodermal *wrt-2* (Mullaney *et al.* 2010; Durieux *et al.* 2011; Taylor and Dillin 2013). *gly-19p*::*kgb-1* and *myo-3p*::*kgb-1* were similarly constructed based on plasmids pNB10 and pPK93_97, respectively, gratefully received from the Dillin laboratory (Durieux *et al.* 2011). KGB-1's coding region was amplified from complementary DNA (cDNA) using forward primers tailed with restriction sites (capitalized) for *Xma*I, for *gly-19p*::*kgb-1* (5′-TCCCCCCGGGatggaagtggatctgccggtacat-3′), or *Bam*HI, for *myo-3p*::*kgb-1*, (5′-CGGGATCCatggaagtggatctgccggtacat-3′),

and the *Eco*RI-tailed reverse primer 5′-CCGGAATTCttatc cagtgaaaatgtcgtggtcgg-3′ (56°), and ligated downstream to the respective promoter and upstream to the *unc-54* 3′-UTR. For neuronal KGB-1, a 3350 bp fragment of the *rgef-1* promoter was excised out of plasmid pNBrgefp (Taylor and Dillin 2013), using *Sph*I and *Xma*I, and inserted into the *gly-19p*::*kgb-1* plasmid, replacing *gly-19p*. Similarly, an epidermal KGB-1 construct was generated by replacing the *gly-19* promoter in the *gly-19p*::*kgb-1* plasmid with 1.6 kb of the *wrt-2* promoter, amplified from genomic DNA using the primers 5′-ACATGCATGCttcagcgcatatacgcccaa-3′ and 5′-TCCCCCCGGG-ccgagaaacaattggcaggttg-3′ (56°), and flanked with restriction sites for *Sph*I and *Xma*I, respectively. Following propagation in *E. coli* DH5α and extraction, plasmids were injected into *kgb-1(km21)* hermaphrodites, in a mix containing 100 ng/μl of the relevant construct as well as 10 ng/μl *myo-2p*::*tdTomato* as an injection marker. Transgenes with the *rgef-1*, *myo-3*, *gly-19*, and *wrt-2* promoters were integrated into the *C. elegans* genome using ionizing irradiation, as described elsewhere (Evans 2006), yielding two independent lines each for intestinal, muscle, and neuronal KGB-1 expression, and a single line for epidermal KGB-1. All lines were backcrossed six times to *kgb-1(km21)* mutants, to remove background mutations, excluding intestinal KGB-1 line A, which was not backcrossed. Unless otherwise mentioned, results for transgenic worms represent *rgef-1p*::*kgb-1* line B for neuronal expression, *myo-3p*::*kgb-1* line A for muscle expression, and *gly-19p*::*kgb-1* line B for intestinal expression.

A similar procedure was employed to obtain worms expressing KGB-1::GFP, which required amplifying the *kgb-1* coding sequence minus its stop codon: the *gly-19* promoter was excised from the *gly-19p*::*kgb-1* plasmid described above using *Sph*I and *Xma*I, and inserted upstream of *gfp* in plasmid pPD95.75 (Boulin *et al.* 2006); *kgb-1* was amplified from cDNA with tailed primers 5′-**tccccccggg**atggaagtggatctgccggtacat-3′ and 5′-**cggggtacc**gctccagtgaaaatgtcgtggtcgg-3′, and following tail excision with *Xma*I and *Kpn*I, was inserted between the promoter and *gfp* to generate *gly-19p*::*kgb-1*::*gfp*. Neuronal and epidermal *kgb-1* constructs were then generated by replacing *gly-19p* with *rgef-1p* or *wrt-2p* excised from their respective plasmids using *Sph*I and *Xma*I. Microinjection was performed as described above, except that injected worms were of the N2 wild-type strain.

To generate strains expressing DAF-16::GFP, or the *cpr-3p*::GFP transcriptional reporter, either lacking KGB-1, or with tissue-specific KGB-1, the strains TJ356 (*daf-16p*::*daf-16*::*gfp*) and BC11429 (*cpr-3p*::*gfp*) were each crossed either to *kgb-1(km21)* mutants or to the neuronal and intestinal *kgb-1* transgenic strains. Interestingly, *daf-16p*::*daf-16*::*gfp*; *kgb-1(km21)* progeny were difficult to obtain. The strain was eventually obtained from *daf-16p*::*daf-16*::*gfp;kgb-1(km-21); rgef-1p*::*kgb-1* heterozygotes, but the desired homozygous progeny presented relatively lower GFP intensity, putatively due to loss of integrated DAF-16::GFP copies, suggesting that *kgb-1* disruption may be synergistically detrimental with DAF-16 overexpression.

All worms were grown at 20°, except where otherwise designated.

Imaging

Worms picked onto slides were paralyzed with 25 mM levamisole (Sigma, St. Louis, MO), and imaged using a Leica MZ16F fluorescent stereoscope (Leica, Wetzlar, Germany) equipped with a MicroPublisher 5.0 RTV (QImaging, BC, Canada). When analysis required quantification of signal intensity, image acquisition used the same settings for all samples in an experiment, followed by quantification of average signal intensity per worm (background-subtracted) using ImageJ (National Institutes of Health, Bethesda, MD).

RNA interference-mediated knockdown

Knockdown by feeding was performed using standard protocols, with clones from the Ahringer RNAi library (Kamath *et al.* 2003), excluding vhp-1 RNA interference (RNAi), which was from the Open Biosystems Library (Reboul *et al.* 2003). Bacteria harboring an empty RNAi vector served as control. Larval knockdown was achieved by exposing worms from the egg stage to larval L4; knockdown in adults was carried out from L4 to day 2 of adulthood, unless otherwise mentioned. All experiments were performed at 20°, unless otherwise mentioned.

Exposure to cdc-25.1 RNAi during development was used to disrupt germline proliferation, as described elsewhere (Shapira and Tan 2008), and to sterilize worms and promote DAF-16 nuclear localization downstream to gonad signaling.

Cadmium-induced gene expression

Eggs were grown on NGM plates until the L4 stage, then transferred to K plates [1.55 g NaCl, 1.19 g KCl, 8.5 g Bacto™ Agar, H2O to 1 litre; sterilized by autoclaving] with or without 1 mM $CdCl_2$ for 1 hr. Worms were then collected and RNA quantified as described below.

Western blot analysis

L4 worms were washed off RNAi plates using M9 buffer and pelleted at 1000 rpm for 3 min. Then, 2× Laemmli sample buffer (Bio-Rad, Hercules, CA) was added to pellets, followed by boiling at 95° for 10 min. Samples were loaded and electrophorated on 4–20% Mini-PROTEAN TGX Precast Protein Gels (Bio-Rad). Protein was transferred to Amersham Hybond-P PVDF membranes (GE Healthcare, Little Chalfont, UK) in 20% methanol transferring buffer at 4° (100 volt for 90 min). Membranes were blocked with 5% BSA in TBST (0.05% Tween 20) for 1 hr and then incubated (overnight at 4°) with rabbit anti–phospho-KGB-1 or anti–KGB-1 antibodies (both gratefully received from Kunihiro Matsumoto, Nagoya, Japan), diluted 1:500 in 5% BSA TBST. Mouse anti-tubulin antibodies (Cell Signaling Technology, Danvers, MA) were used in a 1:1000 dilution, with a 1 hr incubation at 4°. After four washes, membranes were incubated with secondary HRP-conjugated goat anti-rabbit or anti-mouse antibodies (1:5000; Invitrogen, Grand Island, NY). Signal was detected using the Western Lightning ECL Kit (Perkin Elmer, Norwalk,

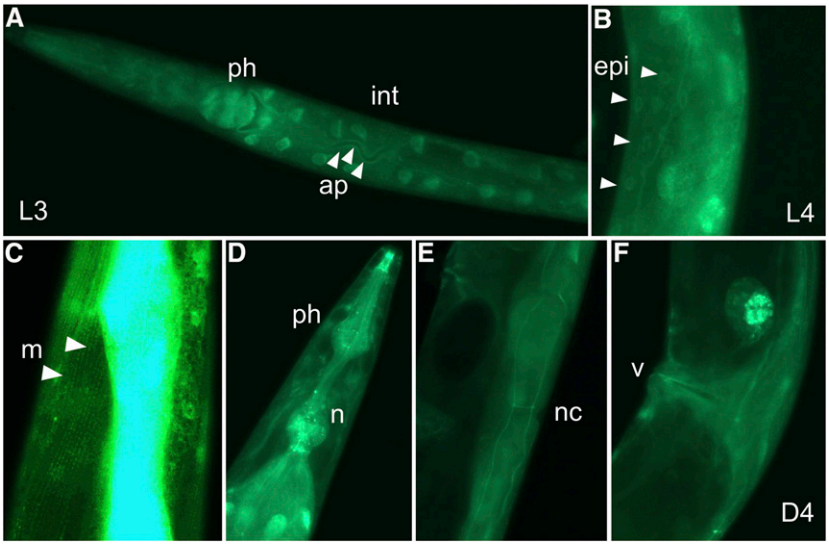

Figure 1 KGB-1 is broadly expressed. Images (not to scale) of *kgb-1p*::*kgb-1*::*gfp* worms from the larval L3 stage to day 4 of adulthood (D4). (A) Pharyngeal (ph) and intestinal (int) expression, with prominent localization to intestinal nuclei and to intestinal cell apical membranes (ap, arrowheads). (B) Epidermal (epi) expression, with arrowheads marking nuclei. (C) Muscle (m) expression; fluorescence intensity is blown up to show association with muscle fibers (arrowheads). (D) Expression in head neurons (n). (E) Expression in neuronal commissures (nc). (F) Vulval (v) expression.

CT), and quantified using ImageJ, using identical region-of-interest frames for band signal density measurements, subtracting local background values, and normalizing phospho-KGB-1 density values to levels of total KGB-1, to facilitate comparisons.

Cadmium and tunicamycin resistance assays

Eggs were added to NGM plates containing 50 μM $CdCl_2$ or 1μg/ml tunicamycin. After 3 days at 20°, worms were counted, and the percentages of worms at different stages, or dead, were calculated. When evaluating gene involvement following RNAi knockdown, exposure to RNAi began with gravid mothers and continued in larvae on RNAi plates that contained both ampicillin and IPTG, for double-strand RNA expression, as well as $CdCl_2$ or tunicamycin.

Survival assays

Survival experiments were carried out at 20°, unless otherwise mentioned. Worms were exposed to RNAi from L4 to day 2 of adulthood, and then transferred to the appropriate plates: NGM plates with 100 μg/ml kanamycin seeded with kanamycin-killed OP50 for life span evaluation, and slow-killing plates for *P. aeruginosa* infection, as previously described (Shapira and Tan 2008). Statistical evaluation of differences between survival curves was performed using Kaplan–Meier analysis, followed by a log-rank test.

Quantitative RT-PCR

Total RNA was extracted from 400 to 500 animals using TRIzol (Invitrogen). RNA was treated with DNase to remove genomic DNA contamination (QIAGEN, Hilden, Germany), and cDNA was synthesized using iScriptTM (Bio-Rad). SYBR Green quantitative (q)RT-PCR was performed using the SsoAdvanced Universal SYBR Green Supermix (Bio-Rad) on a StepOnePlus system (Applied Biosystems, Foster City, CA). Gene-specific threshold cycle (Ct) values were normalized by subtracting the respective values for measurements of actin gene expression. Statistical significance was estimated with a *t*-test based on actin-normalized Ct values. Primer sequences are listed below, all requiring annealing temperature at 60°.

cpr-3 forward: GAGGACACGGATGTATGCCT.
cpr-3 reverse: AGTTTGAATTTCGGTGACGG.
kreg-1 forward: ACCGCCAGTCTATGGAACAC.
kreg-1 reverse: TGATGGTGATGGTGATGTCC.
hsp-43 forward: GAAAGAGAACGACCTGTGGC.
hsp-43 reverse: AATCCTTCCACCAACTGTCG.
mtl-1 forward: GAGGCCAGTGAGAAAAAATGCT.
mtl-1 reverse: GCTCTGCACAATGACAGTTTGC.
actin forward: TCGGTATGGGACAGAAGGAC.
actin reverse: CATCCCAGTTGGTGACGATA.

Data availability

Strains used in this study are available upon request. The authors affirm that all data necessary for confirming the conclusions of the article are present within the article, figures, and tables. Supplemental material available at Figshare: https://doi.org/10.25386/genetics.7159487.v1.

Supplemental Material, File S1, containing all supplemental figures, tables, and associated legends, is available for download through Figshare at: https://doi.org/10.25386/genetics.7159487.v1.

Results

KGB-1 is broadly expressed

A previous study described *kgb-1* expression from 1.77 kb of its upstream sequence in the pharynx, intestine, body wall muscle, spermatheca, and sensory neurons, starting as early as the egg stage and continuing through adulthood (Gerke *et al.* 2014). A KGB-1::GFP fusion protein expressed from a 8.7 kb of the *kgb-1* genomic locus including 4.6 kb of the *kgb-1* upstream sequences and all introns demonstrated

similar expression patterns (Figure 1), and further revealed expression in the epidermis (Figure 1B), vulva (Figure 1F), and in what appear to be motor neurons (Figure 1E). Localization of KGB-1 was prominent in intestinal and epidermal nuclei (Figure 1, A and B), in the apical membrane of intestinal cells (Figure 1A), and along the muscle myofilaments (Figure 1C). No obvious differences were identified in the expression and localization of KGB-1 during development or following exposure to stressors.

Tissue-specific KGB-1 expression differentially contributes to stress protection in larvae

To examine tissue-specific contributions of KGB-1 to stress resistance we used tissue-specific promoters driving KGB-1 expression in the intestine, neurons, body wall muscles, and the epidermis of otherwise mutant *kgb-1(km21)* animals (Figure 2A). Following transgene integration and backcrossing (see *Materials and Methods*), all constructs drove *kgb-1* overexpression, as dictated by their tissue-specific promoters. Correct tissue-specific expression was verified with a separate set of transgenic worms expressing a KGB-1::GFP fusion protein from the same promoters (Figure S1). Subsequent experiments used the transgene set expressing KGB-1 alone, to ensure unaltered function. Indeed, immunoblotting demonstrated that transgenic KGB-1 could be activated in the respective tissues following knockdown of the negative regulator gene *vhp-1*, reportedly expressed in similar tissues as *kgb-1* (Mizuno *et al.* 2004) (Figure 2B). *vhp-1* knockdown resulted in ≥50% increases in levels of phosphorylated KGB-1 in the intestine, muscle, and even in neurons, which are relatively resistant to RNAi-mediated knockdown, but apparently not in the case of *vhp-1* (Figure 2C). Importantly, while *kgb-1* gene expression levels were conspicuously higher in tissue-specific transgenics than in wild-type animals, levels of activated KGB-1, normalized to tubulin, were much closer to those in wild-type animals, suggesting tight control over activated protein levels (Figure 2D). Gross phenotypes associated with *vhp-1* knockdown were also observed in transgenic animals, supporting proper function of transgenic KGB-1. However, phenotypes differed depending on the expressing tissue: activation of neuronal and muscle KGB-1 in L4 worms gave rise to smaller and lighter worms (the latter signifying fewer gut granules), similar to the outcome of *vhp-1* knockdown in wild-type animals; activation of intestinal and epidermal KGB-1 had no obvious effect on worm appearance, as in *kgb-1* mutants (Figure S2), despite the apparent overexpression shown in Figure 2A.

Expression of KGB-1 in neurons, muscle, or epidermis partially rescued development of otherwise *kgb-1* mutants exposed to tunicamycin, a glycosylation inhibitor which causes protein misfolding and ER stress, or to cadmium, a heavy metal associated with ER, as well as with oxidative stress (Gardarin *et al.* 2010; Reiling *et al.* 2011) (Figure 3, A and B). Partial rescue, only slightly above that achieved with neuronal expression, was also observed with KGB-1 expression from its endogenous upstream region (Figure S3). In

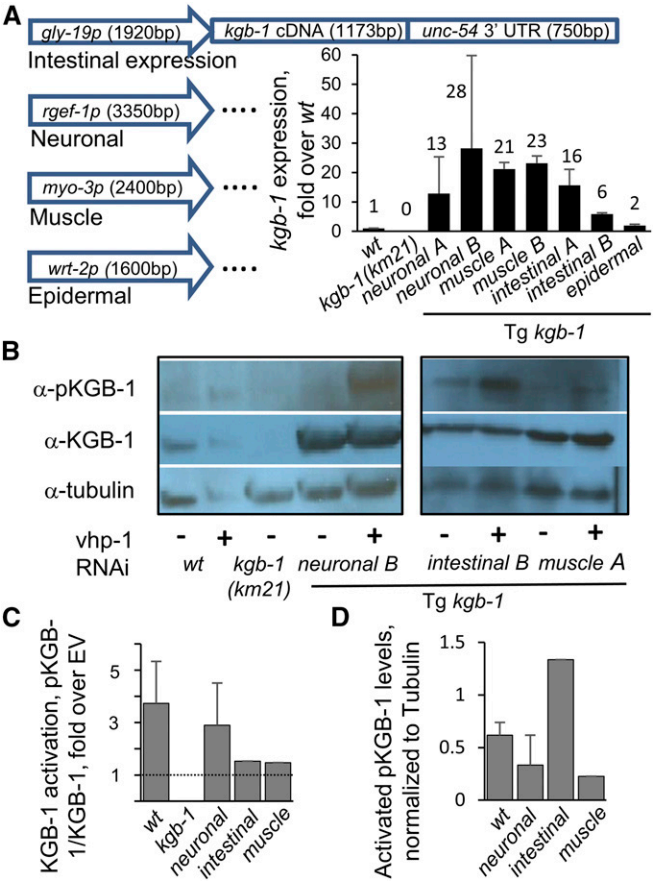

Figure 2 Tissue-specific expression and activation of KGB-1. (A) *kgb-1* tissue-specific expression constructs, and the resulting expression in distinct lines of integrated transgenic (Tg) animals with the *kgb-1(km21)* background; RNA levels were measured in L4 larvae. Averages ± SDs from two to three qRT-PCR experiments, each performed in duplicate. (B) Immunoblotting of protein extracts from L3/L4 larvae, using designated antibodies, demonstrates activation of KGB-1 in either one of the tested expressing tissues following *vhp-1* knockdown. (C and D) Quantification of signal in immunoblots: (C) KGB-1 activation, shown as normalized values in worms treated with vhp-1 RNAi compared to controls; (D) levels of activated KGB-1 in vhp-1 RNAi-treated animals. Values from an additional immunoblot are factored in when available, for the wild-type, *kgb-1* mutants, and the neuronal KGB-1 strains; shown are averages and SDs.

contrast, intestinal KGB-1 expression improved stress resistance only marginally. This was not dependent of transgene integration site, as independently derived transgenic lines showed the same result, *i.e.*, partial, yet significant, rescue of stress resistance with neuronal KGB-1 expression, and marginal contribution with intestinal KGB-1 expression (Figure S4). Furthermore, the extent of contributions did not depend on the extent of KGB-1 overexpression, as distinct integrant lines with 2.3-fold differences in *kgb-1* expression levels within the same tissue presented similar rescuing abilities (Figure 2A and Figure S4). Together, these results provide support for earlier reports suggesting that KGB-1 activation in the epidermis was sufficient to protect worms from heavy metals (Mizuno *et al.* 2008), and expand on these

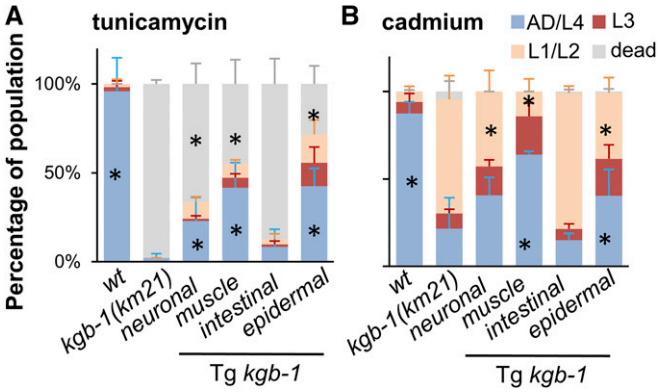

Figure 3 Tissue-specific expression of KGB-1 partially rescues stress resistance in *kgb-1* mutants. Development of worms (3 days at 20°) of designated strains grown in the presence of (A) 1 μg/ml tunicamycin, or (B) 50 μM cadmium. Shown are averages ± SDs for two independent experiments, each performed in duplicates with 100–400 worms per strain per duplicate. * denotes significant differences in the fraction of worms of a developmental stage compared to the respective value in *kgb-1* mutants ($P < 0.05$, *t*-test).

reports to demonstrate that KGB-1 expression in neurons and body wall muscle can provide similar protection. Surprisingly, expression of KGB-1 in the intestine contributed only marginally to protection despite overexpression in this tissue compared to whole-worm endogenous levels, and the fact that some of its gene targets (see below) are expressed in this tissue.

How KGB-1 provides protection from protein folding stress is not known. Activation of the unfolded protein response of the endoplasmic reticulum (UPR^{ER}), represented by induction of the chaperone gene *hsp-4*, was not affected by *kgb-1* disruption, which was further not epistatic to mutations in any of the known UPR^{ER} signaling components (*i.e.*, *xbp-1*, *atf-6*, and *pek-1*), suggesting contribution in parallel (Figure S5). In addition, microarray data mining revealed no induction of the mitochondrial unfolded protein response (UPR^{MT}) by KGB-1 (*i.e.*, expression of *hsp-6* or *hsp-60*) (Zhang *et al.* 2017), indicating that it acted in parallel to mechanisms regulating this response as well.

Differential contributions of tissue-specific KGB-1 is observed also in the detrimental consequences of its activation in adults

KGB-1 is largely known for its role in stress protection. However, previous work showed that in contrast to its protective contributions in developing larvae, its activation in young adults was detrimental, sensitizing worms to protein folding stress, heavy metals, and infection, and shortening life span (Twumasi-Boateng *et al.* 2012). To examine in which tissue KGB-1 activation was the most relevant for these effects, we knocked down *vhp-1* in worms expressing KGB-1 in different tissues, beginning at the L4 stage, and evaluated the outcome of this activation for resistance to *P. aeruginosa* infection and for life span. Similar to larval stress protection, activation of KGB-1 in muscle and in neurons was sufficient to restore the wild-type phenotype, in this case sensitizing adult worms to infection (Figure 4A and Table S1). KGB-1 activation in the intestine gave variable results, but long enough exposure to vhp-1 RNAi (3 days) could sensitize worms to infection.

To complement observations in animals with tissue-specific KGB-1 expression, and to circumvent potential effects of overexpression, we took advantage of *sid-1(qt9)* mutants, lacking a double-strand RNA channel required for systemic RNAi. In this background, rescue with transgenic tissue-specific expression of *sid-1* enables tissue-specific RNAi knockdown (Jose *et al.* 2009; Gelino *et al.* 2016). Using strains allowing intestine-, or neuron-specific *vhp-1* knockdown and tissue specific activation of the endogenous KGB-1, we observed similar outcomes as those described above: KGB-1 activation either in neurons or in the intestine was sufficient to sensitize worms to infection (Figure 4A).

KGB-1 activation in neurons was also very effective in shortening worm life span, while activation of muscle or intestinal KGB-1 had weaker effects (Figure 4B and Table S2). Contrasting with these tissues, KGB-1 activation in the epidermis consistently showed no detrimental effects either on infection resistance, or on life span (Figure 4, A and B).

The results of phenotypic analyses support both cell-autonomous and -nonautonomous contributions of KGB-1 to protecting tissues, or compromising them, under adverse conditions. Epidermal KGB-1 expression provided protection from environmental/external threats in larvae, while intestinal expression sensitized adults to pathogenic/internal stress. In addition to cell-autonomous contributions, muscle, and even more so neuronal KGB-1, demonstrated significant contributions to both protective and detrimental phenotypes.

Cell-autonomous and -nonautonomous contributions of KGB-1 to gene expression

To better distinguish between local- and cross-tissue contributions of KGB-1, we followed the expression of tissue-specific KGB-1 targets. The cathepsin B homolog gene *cpr-3* is expressed mainly in the intestine (and at much lower levels in the pharynx), and was previously shown to be induced by the transcription factor FOS-1 downstream to KGB-1 activation (Zhang *et al.* 2017). Activation of intestinal KGB-1 by *vhp-1* knockdown during development induced expression of a *cpr-3p*::GFP reporter, but not as much as in wild-type animals (Figure 5, A and B). On the other hand, activation of neuronal KGB-1 caused induction comparable to that observed in wild-type animals. In both cases, *cpr-3* induction was dependent on FOS-1 (Figure 5C). Expanding analysis to KGB-1 in additional tissues, and using qRT-PCR to measure endogenous expression, *cpr-3* again showed strong induction following neuronal KGB-1 activation, and a similar induction following activation of muscle KGB-1. In contrast, neither activation of intestinal KGB-1 nor epidermal KGB-1 showed any effect on *cpr-3* expression (Figure 5D). The patterns observed for neuronal and intestinal KGB-1 were recapitulated in independently derived transgenic lines (Figure S6). Similar patterns to those of *cpr-3* were observed with a second

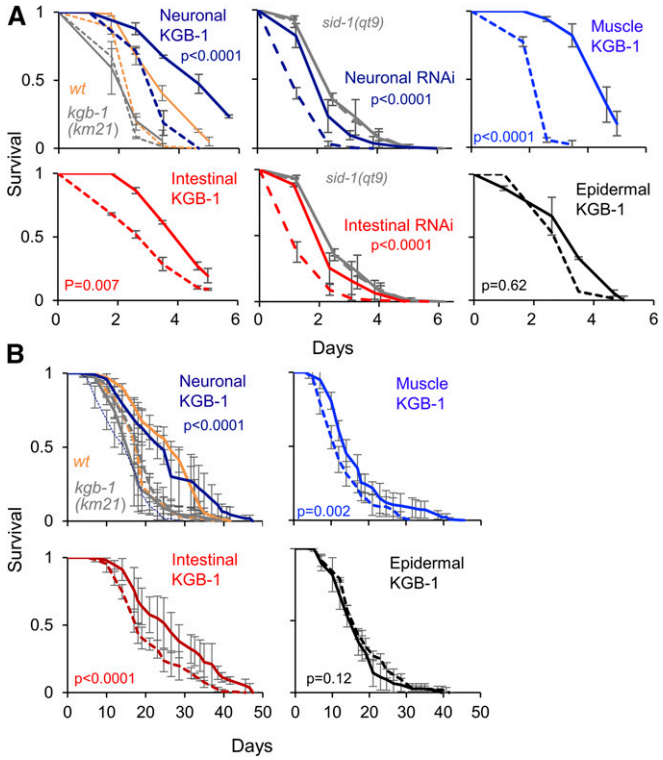

Figure 4 Tissue-specific KGB-1 contributions to detrimental effects in adults. (A) Infection resistance or (B) life span for adults (time 0) of the designated strains, assessed following exposure to control RNAi (solid lines), or vhp-1 RNAi (dashed) for 3 days (in infection experiments with tissue-specific KGB-1 expression shown in A), or for 2 days (in all other panels in A and B). Shown are averages ± SDs of fraction survival measured in triplicates with a total of 38–233 worms per group per experiment (Tables S1 and S2). Shown in each panel is a representative of two to three independent experiments, or a single experiment for tissue-specific RNAi experiments.

KGB-1–dependent intestinal gene, *kreg-1* (Zhang *et al.* 2017) (Figure 5F and Figure S6).

Further examination of *cpr-3* gene expression upon activation of the endogenous KGB-1 through tissue-specific *vhp-1* knockdown in SID-1 transgenics, reasserted its induction by neuronal KGB-1. However, with an intestine-specific RNAi strain, *cpr-3* induction was also observed following intestinal KGB-1 activation, and was comparable to that of wild-type animals (Figure 5E). Thus, whereas the extent of cell-autonomous contributions of KGB-1 to intestinal gene expression remains uncertain, the effects of neuronal KGB-1 activation provide strong support for cell-nonautonomous contributions of extraintestinal KGB-1.

To follow KGB-1-dependent gene expression outside of the intestine, we used *hsp-43*, a KGB-1 target that was previously described to localize to cell-cell junctions, in particular interfaces between epidermis and muscle cells, and is thought to be expressed in the epidermis (Ding and Candido 2000; Zhang *et al.* 2017). Unlike the intestinal genes described above, only epidermal activation of KGB-1 could induce larval *hsp-43* gene expression (Figure 5G). This was observed both in tissue-specific KGB-1 transgenics as well as in tissue-specific RNAi strains, where the disruption of systemic RNAi in *rde-1(ne219)* mutants, rescued with epidermal RDE-1, enabled epidermal-specific *vhp-1* knockdown, resulting in *hsp-43* gene induction comparable to that observed in wild-type animals (Figure 5H). This supported the initial interpretation that *hsp-43* is expressed in the epidermis, and demonstrated that in this case contributions of KGB-1 were uniquely cell autonomous.

Although *vhp-1* knockdown provides an efficient way to activate KGB-1, we wished also to examine KGB-1 activation under physiological conditions. To this end, we exposed wild-type and tissue-specific transgenic *kgb-1* worms to cadmium. Similar to vhp-1 RNAi-dependent KGB-1 activation, we observed only marginal ability of intestinal KGB-1 to induce intestinal gene expression, as represented by *cpr-3* and the intestinal cadmium response gene *lys-3* (Hattori *et al.* 2013) (Figure 5I). In contrast, neuronal KGB-1 was effective in driving intestinal gene induction, supporting a dominant role for neuronal KGB-1 in regulating intestinal expression.

Gene expression and survival analyses combine to demonstrate both cell-autonomous and nonautonomous contributions of KGB-1. In the epidermis, KGB-1 functions cell-autonomously to regulate local gene expression, and provides protection from heavy metals and ER stress, but does not affect resistance to intestinal infection. Conversely, intestinal KGB-1 regulates local intestinal gene expression (albeit variably), and is sufficient to compromise infection resistance and life span in adults, but does not contribute to protein folding and heavy metal stress. Beyond these cell-autonomous contributions, neuronal KGB-1 (as well as muscle KGB-1) strongly activates intestinal gene expression and affects both stress resistance in larvae and infection resistance and life span in adults.

Cell-nonautonomous contributions of KGB-1 to age-dependent DAF-16 regulation

Much of the age-dependent contributions of KGB-1 to stress resistance depend on DAF-16, whose nuclear localization is promoted by KGB-1 activation in larvae, but attenuated in adults (Twumasi-Boateng *et al.* 2012). Therefore, we tested the ability of intestinal and neuronal KGB-1, representing cell-autonomous and-nonautonomous contributions, respectively, to regulate DAF-16. We found that neuronal KGB-1 was as effective as the endogenous KGB-1 in wild-type larvae in driving nuclear localization of DAF-16 in the intestine, while intestinal KGB-1 was far less effective (Figure 6, A and B). To verify this, and to further examine DAF-16 regulation by KGB-1 expressed in additional tissues, we followed the expression of *mtl-1*, an intestinal metallothionein, which is induced in larvae following KGB-1 activation, mediated by DAF-16 (Barsyte *et al.* 2001; Zhang *et al.* 2017). qRT-PCR measurements showed that *mtl-1* could be induced by KGB-1 activation in neurons or muscle, but to a much lesser extent by KGB-1 activation in the intestine or epidermis (Figure 6C).

Attenuation of DAF-16 nuclear localization in adults was examined following *cdc-25.1* knockdown, which impairs germline proliferation, activating gonadal hormone signaling

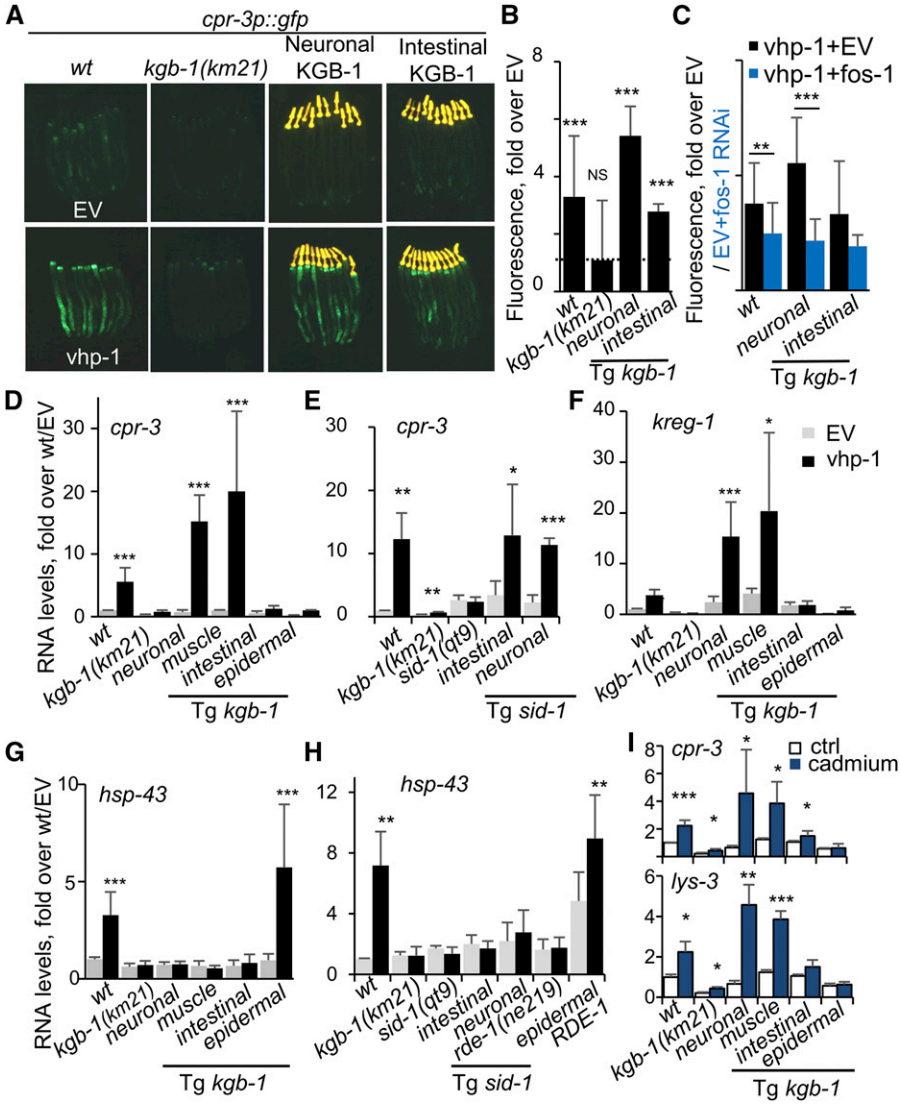

Figure 5 Cell-autonomous and -nonautonomous effects of KGB-1 activation on gene expression. (A) Representative images of L4 *cpr-3p*::*gfp* transgenics, with wild-type genetic background, *kgb-1(km21)*, or tissue-specific KGB-1, fed throughout development with control (EV), or vhp-1 RNAi. Images were acquired using identical magnification and exposure settings. (B) Quantification of GFP signal. Averages ± SDs for two independent experiments (n = 9–11 worms per group per experiment). (C) Quantification of similar experiments as in B, with egg to young adult exposure to RNAi mixtures, as designated; cdc-25.1 RNAi was additionally included in all RNAi mixes, to abolish differences associated with selective sterility, previously shown for *fos-1* knockdown; previous work showed that mixtures of the RNAi clones in use gave rise to efficient knockdown (Zhang *et al.* 2017). Shown are averages ± SDs (wild-type, n = 24–31 worms per group; neuronal, n = 16–19 worms per group; intestinal, n = 7–15 worms per group; * $P < 0.05$, ** $P < 0.01$, *** $P < 0.001$, t-test). (D–I) qRT-PCR measurements of gene induction in L4 larvae following KGB-1 activation by (D–H) *vhp-1* knockdown (D–H), or exposure to cadmium (1 mM, 1 hr); tissue-specificity was achieved through restricted expression of KGB-1 or RNAi machinery in the designated mutants. Averages ± SDs for measurements from two to three independent experiments, each measured in duplicates. Asterisks mark significant induction following *vhp-1* knockdown or cadmium treatment (* $P < 0.05$, ** $P < 0.01$, *** $P < 0.001$, paired t-test).

and driving DAF-16 nuclear localization in sterile animals (Berman and Kenyon 2006; Shapira and Tan 2008). Previous work has shown that cdc-25.1-RNAi did not affect KGB-1's contributions (Twumasi-Boateng *et al.* 2012). Following this treatment, *vhp-1* knockdown reproducibly reduced the fraction of worms showing nuclear DAF-16 by 5.6-fold (Figure 6, D and E). Both neuronal and intestinal KGB-1 were capable of recapitulating this effect, although the variability in the initial effects of cdc-25.1 RNAi resulted in reduced statistical significance for some of the groups (Figure 6E). qRT-PCR measurements of *mtl-1*, showing lower variability, confirmed the overall trend and further highlighted the smaller contribution of intestinal KGB-1 compared to that of neuronal and muscle KGB-1 (Figure 6F). Epidermal KGB-1 showed no significant contribution to DAF-16 attenuation. These results further emphasize the dominance of cell-nonautonomous contributions of KGB-1, in which KGB-1 activation in neurons and muscle was more potent in regulating intestinal DAF-16 outputs than local KGB-1 activation.

Mediation of cell-nonautonomous contributions of KGB-1

Our results showed that KGB-1 activation in different tissues contributed to intestinal gene expression and to KGB-1–dependent phenotypes in a cell-nonautonomous manner. Focusing on the effects of neuronal KGB-1, we examined the involvement of vesicle secretion in mediating intertissue communication, aiming to distinguish between secretion of classical neurotransmitters and neuropeptides. To this end, we tested the involvement of *unc-13*, which is important for synaptic transmission of small clear vesicles, particularly relevant for the secretion of neurotransmitters such as acetylcholine and GABA (Richmond *et al.* 1999), and *unc-31*, which is specifically important for the secretion of dense core vesicles, carrying neuropeptides and monoamines (Speese *et al.* 2007). Although disruption of *unc-31* did not affect induction of *cpr-3p*::*gfp* following activation of neuronal KGB-1, disruption of *unc-13* reduced it by more than twofold (Figure 7, A and B and Figure S7). This was confirmed by qRT-PCR

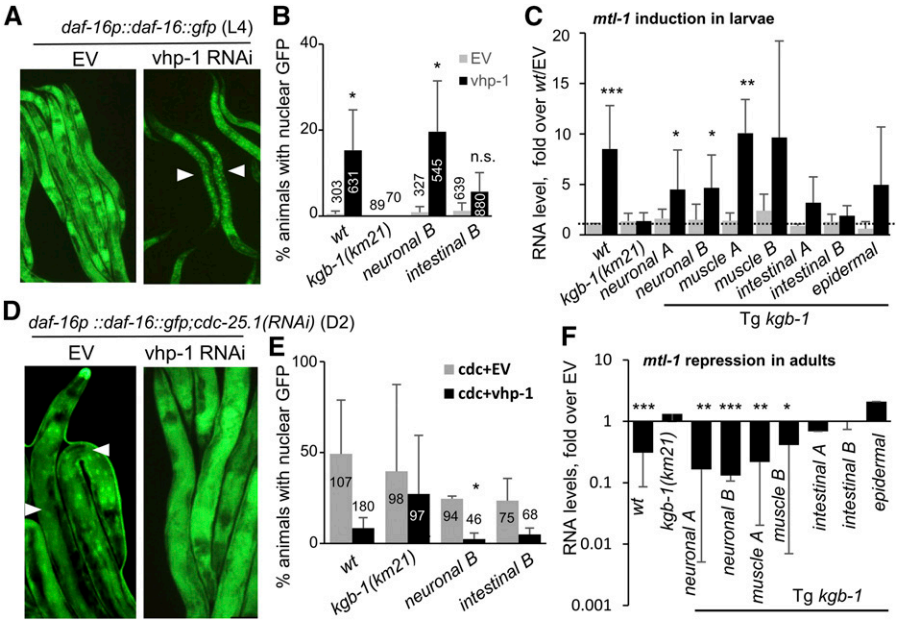

Figure 6 KGB-1 regulates DAF-16 cell-nonautonomously. (A and D) Representative images showing DAF-16::GFP nuclear localization in (A) wild-type L4 or (D) day 2 adults following 2 days of exposure to RNAi as designated, and further including cdc-25.1 RNAi in the experiment shown in D, to drive DAF-16 nuclear localization. Arrowheads mark worms with nuclear localization. (B) Quantification of DAF-16::GFP nuclear localization in L4 worms of the designated genetic backgrounds. Averages ± SDs of three independent experiments, each with 20–380 worms per group (*N* shown on columns). (C) qRT-PCR measurements of *mtl-1* gene induction following *vhp-1* knockdown in larvae expressing tissue-specific KGB-1. Averages ± SDs for two to nine independent experiments, each measured in duplicates. (E) DAF-16 nuclear localization quantified as in B, in day 2 adult worms treated during development with cdc-25.1 RNAi, and then shifted to cdc-25.1+EV or vhp-1 RNAi; averages of two experiments, each with $N = 21$–92 per group. (F) qRT-PCR measurements in day 2 adults; shown is fold repression relative to values in the respective EV-treated worms. Averages ± SDs for two to five independent experiments for each strain, each measured in duplicates. Asterisks mark significant induction following *vhp-1* knockdown. * $P < 0.05$, ** $P < 0.01$, *** $P < 0.001$; *t*-test for nuclear localization, paired *t*-test for qRT-PCR measurements.

measurements of endogenous *cpr-3* gene expression (Figure 7C). These findings suggest that neurotransmission from neurons to the intestine is involved in mediating the contributions of KGB-1. This is probably not the only mode through which KGB-1 relays stress signals to the intestine, as KGB-1 activation in nonneuronal tissues, which do not express *unc-13*, must rely on other mechanisms.

Discussion

Our examination of tissue-specific contributions of KGB-1 to gene expression, stress resistance, and life span reveals both cell-autonomous and -nonautonomous inputs. In the epidermis, cell-autonomous contributions played a significant role in stress resistance and gene expression. In the intestine, cell-autonomous KGB-1 activation contributed to local gene expression (albeit with variable efficiency) and to compromised survival, but cell-nonautonomous inputs from neuronal and muscle KGB-1 further played a significant role, both in gene regulation and in stress resistance. Nonautonomous contributions of neuronal KGB-1 were observed both in strains expressing transgenic KGB-1 from a panneuronal promoter, as well as in worms enabling neuronal-specific activation of the endogenous KGB-1, which seems to be expressed only in a subset of neurons. It should be noted that KGB-1 may be expressed in more tissues than those identified with its 4.6 kb upstream sequence (and the KGB-1::GFP reporter), as rescue of wild-type resistance to cadmium and tunicamycin was only partial in worms expressing KGB-1 from this promoter (Figure S3), suggesting that additional inputs are required for full rescue. Intriguingly, the results from KGB-1 transgenic animals showed that regulation of intestinal KGB-1 targets by extraintestinal KGB-1 activation did not depend on intestinal KGB-1 (although it did depend on the KGB-1 downstream transcription factor FOS-1). The signal provided by extraintestinal KGB-1 to regulate FOS-1–dependent gene expression or DAF-16 nuclear localization is not known, but the requirement for *unc-13* suggests that neurotransmission takes some part in this communication.

Unlike epidermal and neuronal KGB-1 activation, which showed consistent patterns of gene induction both in tissue-specific KGB-1 transgenic strains and in tissue-specific RNAi strains, analysis of the role played by intestinal KGB-1 provided conflicting results: in KGB-1 transgenic animals, intestinal KGB-1 activation caused a relatively small induction of GFP expression from the *cpr-3* promoter, or no induction at all of the endogenous *cpr-3*; in contrast, *vhp-1* RNAi-mediated intestinal activation of the endogenous KGB-1 in *sid-1;vha-6p*::*sid-1* animals induced *cpr-3* gene expression similar to KGB-1 activation in neurons. While the cause for this discrepancy is not known, one possible explanation is the potential of vhp-1 RNAi, once it is taken up by intestinal cells, to reach neurons independently of SID-1 and activate the neuronal KGB-1. Neuronal resistance to RNAi is thought to be largely due to the lack of SID-1 expression in these cells; however, the ability to enhance neuronal RNAi by disrupting other genes, such as *eri-1*, encoding a neuronal exonuclease, indicates that RNAi can be taken up independently of SID-1 (Grishok 2005; Calixto *et al.* 2010). Once inside neurons, vhp-1 RNAi could activate KGB-1, as demonstrated by our Western blot results (Figure 2), compromising the intended specificity of KGB-1 activation in the intestinal SID-1 strain.

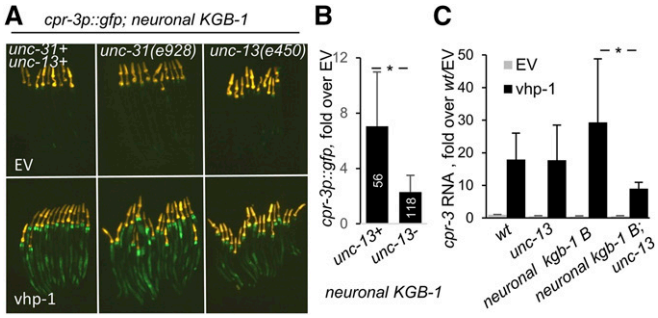

Figure 7 Disruption of neuronal secretion impairs cell-nonautonomous contributions of neuronal KGB-1 (A). Intestinal gene induction in L4 larvae following vhp-1 RNAi-mediated activation of neuronal KGB-1, in animals with the designated genetic backgrounds. (B) Quantification of GFP signal in animals with only neuronal KGB-1. Averages ± SDs of values in three independent experiments with N = 9–30 worms per group per experiment; N shown on columns ($P = 1.7 \times 10^{-24}$, t-test). (C) qRT-PCR measurements of endogenous *cpr-3* induction following KGB-1 activation in L4 larvae of the designated strains. Averages ± SDs for measurements from two independent experiments, each measured in duplicates; * $P <$ 0.01, t-test.

Besides the results from the intestine-specific RNAi strain, all others indicate a relatively minor contribution of intestinal KGB-1 to gene expression and stress protection, including (1) lack of induction of intestinal gene targets, either following vhp-1 RNAi-mediated KGB-1 activation, or cadmium exposure; and (2) smaller contributions (compared to those of neuronal KGB-1 activation) to life span shortening and infection susceptibility in adults (to see the latter effect, vhp-1 RNAi exposure had to be prolonged to 3 days instead of the standard 2-day exposure; see Table S1). The small yet significant increase in GFP expression from the *cpr-3* promoter following activation of intestinal KGB-1 (Figure 5A) could further be attributed to increased copy number of both KGB-1 and its target, potentially amplifying an otherwise weak effect. Taken together, the results support some cell-autonomous contribution of intestinal KGB-1, but suggest that this contribution might be small compared to cell-nonautonomous contributions of extraintestinal KGB-1.

Cell-nonautonomous responses to stress have been previously described in *C. elegans*. Protein aggregation in neurons was shown to activate the intestinal UPR^{MT}, which required *unc-31*, and the neurotransmitter serotonin (Berendzen *et al.* 2016). Similarly, the UPR^{ER} was also shown to be activated through cell-nonautonomous responses, but this activation depended on *unc-13* and not *unc-31* (Taylor and Dillin 2013). In addition, a noncanonical branch of the UPR^{ER} was found to be activated nonautonomously during infection, through stimulation of neurons expressing the G-protein–coupled receptor OCTR-1 (Sun *et al.* 2011). Thus, there might be more than one secreted factor that mediate cell-nonautonomous stress responses. In addition, nonneuronal signaling can also contribute to nonautonomous stress responses, as demonstrated by transcellular chaperone signaling, in which the HSP90 gene *hsp-90/daf-21*, induced in muscle cells under protein folding stress, promoted enhanced proteostasis in other tissues (van Oosten-Hawle *et al.* 2013). Cell-nonautonomous contributions are also observed in the function of *C. elegans* insulin signaling. Activation of the transcription factor DAF-16 in the intestine was shown to increase DAF-16–dependent gene expression in other tissues, which was mediated by the insulin-like peptide *ins-7* and was termed *DAF-16-to-DAF-16* transmission (Libina *et al.* 2003; Murphy *et al.* 2007); in addition, DAF-16–dependent gene expression could also be activated without local DAF-16, which was found to depend on MDT-15 (Zhang *et al.* 2013).

The characteristics of KGB-1's cell-nonautonomous contributions overlap to some extent with those of the UPR^{ER}, in the sense that both help mitigate similar adverse conditions, and both depend on *unc-13*–mediated signaling. However, our results clearly demonstrate that KGB-1 was not required for the UPR^{ER} and that its contributions were different from (and additive to) those of UPR^{ER} signaling. Nevertheless, it is possible that the two pathways share signals to activate complementary stress responses. Moreover, KGB-1 activation in nonneuronal tissues, particularly muscle, lacking *unc-13* expression, also demonstrated cell-nonautonomous contributions, suggesting existence of additional signaling mechanisms. Further insight into mechanisms responsible for both neuronal and nonneuronal contributions of KGB-1 may be offered by our finding that KGB-1 regulated DAF-16 nonautonomously. This may suggest additional mechanisms, not necessarily mutually exclusive with those thought to be involved in UPR^{ER} signaling. Similar to *DAF-16-to-DAF-16* signaling, INS-7 secretion may be involved in signal propagation downstream to KGB-1 activation in nonneuronal tissues. With respect to neuronal contributions, a previous study reported effects of GABAergic signaling in a subset of motor neurons on DAF-16 regulation, which suggests involvement of GABAergic neurotransmission in propagating neuronal signals of KGB-1 activation (Chun *et al.* 2015); this possibility is further supported by the observed expression of KGB-1 in putative motor neurons, as well as by its reported importance for axon regeneration in such neurons (Pastuhov *et al.* 2012). Lastly, it does not appear unlikely that the mechanisms proposed so far are associated with cellular surveillance. Surveillance mechanisms were previously shown to monitor the organism for disruption of essential functions, such as protein translation or proteolysis, and activate immune and detoxification responses in tissues other than those affected (Melo and Ruvkun 2012; Lehrbach and Ruvkun 2016). Importantly, KGB-1 was found to be central in activating these responses. While these responses are protective, KGB-1 activation in adults, as part of the cellular surveillance, was found to be detrimental for activation of the UPR^{MT} (Runkel *et al.* 2013). This presents an intriguing parallel to the functional switch that we identified for KGB-1 and further corroborates the possibility that cell-nonautonomous contributions of KGB-1 represent its roles in cellular surveillance.

Integration of stress signaling at the level of the whole organism seems to fall within the sphere of cellular

surveillance. In this capacity, KGB-1 may help protect the organism and enable resource allocation. However, as our results suggest [as well as results from others, see Runkel *et al.* (2013)], in adults this may have detrimental consequences, and could link adverse environmental conditions to accelerated aging. The age-dependent reversal in the outcome of KGB-1 activation has the characteristics of antagonistic pleiotropy, in which a gene's contribution is beneficial early in life, but detrimental later: positively selected for its beneficial contributions, but affecting aging due to its detrimental contributions (Williams 1957). Understanding antagonistic pleiotropy can thus shed light on aging. Our results suggest that the antagonistic pleiotropy presented by KGB-1 depends significantly on its activation in neurons.

The significance of the described findings likely goes beyond *C. elegans*. Cell-nonautonomous contributions to health, both positive and negative, have been described also in vertebrates. On the positive side, murine expression of the spliced and activated form of the UPR^{ER} regulator XBP1 in hypothalamic neurons was shown to increase hepatic insulin sensitivity, even under conditions that otherwise promote insulin resistance (Williams *et al.* 2014). On the negative side, secretion from senescing cells was shown to promote pathology in neighboring cells, as well as systemic inflammation, contributing to aging phenotypes (Childs *et al.* 2015). Such observations highlight the need for a better understanding of how stress signals are integrated and what are the consequences of such integration for stress resistance and aging.

Acknowledgments

We thank Kunihiro Matsumoto, Malene Hansen, Alex Soukas, Andrew Dillin, and Barbara Meyer, and members of their laboratories (in particular Ye Tian and Denise Matsubara) for help with strains and reagents, and further thank Ye Tian and Andrew Dillin for useful comments, and Maya Para and Medha Somayaji for last minute help. Work presented in this manuscript was funded by the National Science Foundation division of Integrative Organismal systems (grant 1355240). C.R. was further supported by a Berkeley Undergraduate Research Apprentice Program fellowship.

Literature Cited

Barsyte, D., D. A. Lovejoy, and G. J. Lithgow, 2001 Longevity and heavy metal resistance in daf-2 and age-1 long-lived mutants of Caenorhabditis elegans. FASEB J. 15: 627–634. https://doi.org/10.1096/fj.99-0966com

Berendzen, K. M., J. Durieux, L. W. Shao, Y. Tian, H. E. Kim *et al.*, 2016 Neuroendocrine coordination of mitochondrial stress signaling and proteostasis. Cell 166: 1553–1563.e10. https://doi.org/10.1016/j.cell.2016.08.042

Berman, J. R., and C. Kenyon, 2006 Germ-cell loss extends C. elegans life span through regulation of DAF-16 by kri-1 and lipophilic-hormone signaling. Cell 124: 1055–1068. https://doi.org/10.1016/j.cell.2006.01.039

Block, D. H., K. Twumasi-Boateng, H. S. Kang, J. A. Carlisle, A. Hanganu *et al.*, 2015 The developmental intestinal regulator ELT-2 controls p38-dependent immune responses in adult C. elegans. PLoS Genet. 11: e1005265. https://doi.org/10.1371/journal.pgen.1005265

Boulin, T., J. F. Etchberger, and O. Hobert, 2006 Reporter gene fusions, (April 5, 2006), *WormBook*, ed. The *C. elegans* Research Community, WormBook, doi/10.1895/wormbook.1.106.1, http://www.wormbook.org.

Calixto, A., D. Chelur, I. Topalidou, X. Chen, and M. Chalfie, 2010 Enhanced neuronal RNAi in C. elegans using SID-1. Nat. Methods 7: 554–559. https://doi.org/10.1038/nmeth.1463

Childs, B. G., M. Durik, D. J. Baker, and J. M. van Deursen, 2015 Cellular senescence in aging and age-related disease: from mechanisms to therapy. Nat. Med. 21: 1424–1435. https://doi.org/10.1038/nm.4000

Chun, L., J. Gong, F. Yuan, B. Zhang, H. Liu *et al.*, 2015 Metabotropic GABA signalling modulates longevity in C. elegans. Nat. Commun. 6: 8828. https://doi.org/10.1038/ncomms9828

Ding, L., and E. P. Candido, 2000 Association of several small heat-shock proteins with reproductive tissues in the nematode Caenorhabditis elegans. Biochem. J. 351: 13–17. https://doi.org/10.1042/bj3510013

Durieux, J., S. Wolff, and A. Dillin, 2011 The cell-non-autonomous nature of electron transport chain-mediated longevity. Cell 144: 79–91. https://doi.org/10.1016/j.cell.2010.12.016

Evans, T. C., 2006 Transformation and microinjection, (April 6, 2006), *WormBook*, ed. The *C. elegans* Research Community, WormBook. https://doi.org/doi/10.1895/wormbook.1.108.1, http://www.wormbook.org.

Gardarin, A., S. Chedin, G. Lagniel, J. C. Aude, E. Godat *et al.*, 2010 Endoplasmic reticulum is a major target of cadmium toxicity in yeast. Mol. Microbiol. 76: 1034–1048. https://doi.org/10.1111/j.1365-2958.2010.07166.x

Gelino, S., J. T. Chang, C. Kumsta, X. She, A. Davis *et al.*, 2016 Intestinal autophagy improves healthspan and longevity in C. elegans during dietary restriction. PLoS Genet. 12: e1006135 (erratum: PLoS Genet. 12: e1006271). https://doi.org/10.1371/journal.pgen.1006135

Gerke, P., A. Keshet, A. Mertenskotter, and R. J. Paul, 2014 The JNK-like MAPK KGB-1 of Caenorhabditis elegans promotes reproduction, lifespan, and gene expressions for protein biosynthesis and germline homeostasis but interferes with hyperosmotic stress tolerance. Cell. Physiol. Biochem. 34: 1951–1973. https://doi.org/10.1159/000366392

Grishok, A., 2005 RNAi mechanisms in Caenorhabditis elegans. FEBS Lett. 579: 5932–5939. https://doi.org/10.1016/j.febslet.2005.08.001

Hattori, A., T. Mizuno, M. Akamatsu, N. Hisamoto, and K. Matsumoto, 2013 The Caenorhabditis elegans JNK signaling pathway activates expression of stress response genes by derepressing the Fos/HDAC repressor complex. PLoS Genet. 9: e1003315. https://doi.org/10.1371/journal.pgen.1003315

Inoue, H., N. Hisamoto, J. H. An, R. P. Oliveira, E. Nishida *et al.*, 2005 The C. elegans p38 MAPK pathway regulates nuclear localization of the transcription factor SKN-1 in oxidative stress response. Genes Dev. 19: 2278–2283. https://doi.org/10.1101/gad.1324805

Jose, A. M., J. J. Smith, and C. P. Hunter, 2009 Export of RNA silencing from C. elegans tissues does not require the RNA channel SID-1. Proc. Natl. Acad. Sci. USA 106: 2283–2288. https://doi.org/10.1073/pnas.0809760106

Kamath, R. S., A. G. Fraser, Y. Dong, G. Poulin, R. Durbin *et al.*, 2003 Systematic functional analysis of the Caenorhabditis

elegans genome using RNAi. Nature 421: 231–237. https://doi.org/10.1038/nature01278

Kim, D. H., R. Feinbaum, G. Alloing, F. E. Emerson, D. A. Garsin *et al.*, 2002 A conserved p38 MAP kinase pathway in Caenorhabditis elegans innate immunity. Science 297: 623–626.

Kim, D. H., N. T. Liberati, T. Mizuno, H. Inoue, N. Hisamoto *et al.*, 2004 Integration of Caenorhabditis elegans MAPK pathways mediating immunity and stress resistance by MEK-1 MAPK kinase and VHP-1 MAPK phosphatase. Proc. Natl. Acad. Sci. USA 101: 10990–10994. https://doi.org/10.1073/pnas.0403546101

Kyriakis, J. M., and J. Avruch, 2001 Mammalian mitogen-activated protein kinase signal transduction pathways activated by stress and inflammation. Physiol. Rev. 81: 807–869. https://doi.org/10.1152/physrev.2001.81.2.807

Lehrbach, N. J., and G. Ruvkun, 2016 Proteasome dysfunction triggers activation of SKN-1A/Nrf1 by the aspartic protease DDI-1. eLife 5: e17721. https://doi.org/10.7554/eLife.17721

Libina, N., J. R. Berman, and C. Kenyon, 2003 Tissue-specific activities of C. elegans DAF-16 in the regulation of lifespan. Cell 115: 489–502. https://doi.org/10.1016/S0092-8674(03)00889-4

Melo, J. A., and G. Ruvkun, 2012 Inactivation of conserved C. elegans genes engages pathogen- and xenobiotic-associated defenses. Cell 149: 452–466. https://doi.org/10.1016/j.cell.2012.02.050

Mizuno, T., N. Hisamoto, T. Terada, T. Kondo, M. Adachi *et al.*, 2004 The Caenorhabditis elegans MAPK phosphatase VHP-1 mediates a novel JNK-like signaling pathway in stress response. EMBO J. 23: 2226–2234. https://doi.org/10.1038/sj.emboj.7600226

Mizuno, T., K. Fujiki, A. Sasakawa, N. Hisamoto, and K. Matsumoto, 2008 Role of the Caenorhabditis elegans Shc adaptor protein in the c-Jun N-terminal kinase signaling pathway. Mol. Cell. Biol. 28: 7041–7049. https://doi.org/10.1128/MCB.00938-08

Mullaney, B. C., R. D. Blind, G. A. Lemieux, C. L. Perez, I. C. Elle *et al.*, 2010 Regulation of C. elegans fat uptake and storage by acyl-CoA synthase-3 is dependent on NR5A family nuclear hormone receptor nhr-25. Cell Metab. 12: 398–410. https://doi.org/10.1016/j.cmet.2010.08.013

Murphy, C. T., S. J. Lee, and C. Kenyon, 2007 Tissue entrainment by feedback regulation of insulin gene expression in the endoderm of Caenorhabditis elegans. Proc. Natl. Acad. Sci. USA 104: 19046–19050. https://doi.org/10.1073/pnas.0709613104

Pastuhov, S. I., K. Fujiki, P. Nix, S. Kanao, M. Bastiani *et al.*, 2012 Endocannabinoid-Goα signalling inhibits axon regeneration in Caenorhabditis elegans by antagonizing Gqα-PKC-JNK signalling. Nat. Commun. 3: 1136. https://doi.org/10.1038/ncomms2136

Reboul, J., P. Vaglio, J. F. Rual, P. Lamesch, M. Martinez *et al.*, 2003 C. elegans ORFeome version 1.1: experimental verification of the genome annotation and resource for proteome-scale protein expression. Nat. Genet. 34: 35–41. https://doi.org/10.1038/ng1140

Reiling, J. H., C. B. Clish, J. E. Carette, M. Varadarajan, T. R. Brummelkamp *et al.*, 2011 A haploid genetic screen identifies the major facilitator domain containing 2A (MFSD2A) transporter as a key mediator in the response to tunicamycin. Proc. Natl. Acad. Sci. USA 108: 11756–11765. https://doi.org/10.1073/pnas.1018098108

Richmond, J. E., W. S. Davis, and E. M. Jorgensen, 1999 UNC-13 is required for synaptic vesicle fusion in C. elegans. Nat. Neurosci. 2: 959–964. https://doi.org/10.1038/14755

Runkel, E. D., S. Liu, R. Baumeister, and E. Schulze, 2013 Surveillance-activated defenses block the ROS-induced mitochondrial unfolded protein response. PLoS Genet. 9: e1003346 [corrigenda: PLoS Genet. 12: e1006377 (2016)]. https://doi.org/10.1371/journal.pgen.1003346

Shapira, M., and M. W. Tan, 2008 Genetic analysis of Caenorhabditis elegans innate immunity. Methods Mol. Biol. 415: 429–442. https://doi.org/10.1007/978-1-59745-570-1_25

Speese, S., M. Petrie, K. Schuske, M. Ailion, K. Ann *et al.*, 2007 UNC-31 (CAPS) is required for dense-core vesicle but not synaptic vesicle exocytosis in Caenorhabditis elegans. J. Neurosci. 27: 6150–6162. https://doi.org/10.1523/JNEUROSCI.1466-07.2007

Sun, J., V. Singh, R. Kajino-Sakamoto, and A. Aballay, 2011 Neuronal GPCR controls innate immunity by regulating noncanonical unfolded protein response genes. Science 332: 729–732. https://doi.org/10.1126/science.1203411

Taylor, R. C., and A. Dillin, 2013 XBP-1 is a cell-nonautonomous regulator of stress resistance and longevity. Cell 153: 1435–1447. https://doi.org/10.1016/j.cell.2013.05.042

Twumasi-Boateng, K., and M. Shapira, 2012 Dissociation of immune responses from pathogen colonization supports pattern recognition in C. elegans. PLoS One 7: e35400. https://doi.org/10.1371/journal.pone.0035400

Twumasi-Boateng, K., T. W. Wang, L. Tsai, K. H. Lee, A. Salehpour *et al.*, 2012 An age-dependent reversal in the protective capacities of JNK signaling shortens Caenorhabditis elegans lifespan. Aging Cell 11: 659–667. https://doi.org/10.1111/j.1474-9726.2012.00829.x

Uno, M., S. Honjoh, M. Matsuda, H. Hoshikawa, S. Kishimoto *et al.*, 2013 A fasting-responsive signaling pathway that extends life span in C. elegans. Cell Rep. 3: 79–91. https://doi.org/10.1016/j.celrep.2012.12.018

van Oosten-Hawle, P., R. S. Porter, and R. I. Morimoto, 2013 Regulation of organismal proteostasis by transcellular chaperone signaling. Cell 153: 1366–1378. https://doi.org/10.1016/j.cell.2013.05.015

Walsh, D. M., and D. J. Selkoe, 2016 A critical appraisal of the pathogenic protein spread hypothesis of neurodegeneration. Nat. Rev. Neurosci. 17: 251–260. https://doi.org/10.1038/nrn.2016.13

Williams, G. C., 1957 Pleiotropy, natural selection, and the evolution of senescence. Evolution (N. Y.) 11: 398. https://doi.org/10.2307/2406060

Williams, K. W., T. Liu, X. Kong, M. Fukuda, Y. Deng *et al.*, 2014 Xbp1s in pomc neurons connects ER stress with energy balance and glucose homeostasis. Cell Metab. 20: 471–482. https://doi.org/10.1016/j.cmet.2014.06.002

Winterbourn, C. C., A. J. Kettle, and M. B. Hampton, 2016 Reactive oxygen species and neutrophil function. Annu. Rev. Biochem. 85: 765–792. https://doi.org/10.1146/annurev-biochem-060815-014442

Zhang, P., M. Judy, S. J. Lee, and C. Kenyon, 2013 Direct and indirect gene regulation by a life-extending FOXO protein in C. elegans: roles for GATA factors and lipid gene regulators. Cell Metab. 17: 85–100. https://doi.org/10.1016/j.cmet.2012.12.013

Zhang, Z., L. Liu, K. Twumasi-Boateng, D. H. S. Block, and M. Shapira, 2017 FOS-1 functions as a transcriptional activator downstream of the C. elegans JNK homolog KGB-1. Cell Signal. 30: 1–8. https://doi.org/10.1016/j.cellsig.2016.11.010

Communicating editor: B. Goldstein